

Seasonal and Regional Manifestation of Arctic Sea Ice Loss

INGRID H. ONARHEIM, TOR ELDEVIK, AND LARS H. SMEDSRUD

Geophysical Institute, University of Bergen, and Bjerknnes Centre for Climate Research, Bergen, Norway

JULIENNE C. STROEVE

University College London, London, United Kingdom, and National Snow and Ice Data Center, Boulder, Colorado

(Manuscript received 24 June 2017, in final form 14 March 2018)

ABSTRACT


The Arctic Ocean is currently on a fast track toward seasonally ice-free conditions. Although most attention has been on the accelerating summer sea ice decline, large changes are also occurring in winter. This study assesses past, present, and possible future change in regional Northern Hemisphere sea ice extent throughout the year by examining sea ice concentration based on observations back to 1950, including the satellite record since 1979. At present, summer sea ice variability and change dominate in the perennial ice-covered Beaufort, Chukchi, East Siberian, Laptev, and Kara Seas, with the East Siberian Sea explaining the largest fraction of September ice loss (22%). Winter variability and change occur in the seasonally ice-covered seas farther south: the Barents Sea, Sea of Okhotsk, Greenland Sea, and Baffin Bay, with the Barents Sea carrying the largest fraction of loss in March (27%). The distinct regions of summer and winter sea ice variability and loss have generally been consistent since 1950, but appear at present to be in transformation as a result of the rapid ice loss in all seasons. As regions become seasonally ice free, future ice loss will be dominated by winter. The Kara Sea appears as the first currently perennial ice-covered sea to become ice free in September. Remaining on currently observed trends, the Arctic shelf seas are estimated to become seasonally ice free in the 2020s, and the seasonally ice-covered seas farther south to become ice free year-round from the 2050s.

1. Introduction

The rapid decline of Arctic sea ice is one of the clearest indicators of ongoing climate change (Serreze and Barry 2011). Along with reduced sea ice cover in both extent and thickness (Kwok and Rothrock 2009; Cavalieri and Parkinson 2012), the multiyear ice cover is decreasing (Maslanik et al. 2007; Nghiem et al. 2007), the melt season is extending (Stroeve et al. 2014), and drift speeds and deformation rates are increasing (Rampal et al. 2009). The current Arctic sea ice transition from a thick, strong ice pack to a thinner, more fragile ice cover affects the marine Arctic ecosystems, possibly alters weather conditions and climate (e.g.,

Honda et al. 2009; Francis and Vavrus 2012), and increases the interest for commercial maritime activity in the Arctic (Emmerson and Lahn 2012). Understanding the changing Arctic sea ice cover is thus of scientific and practical urgency.

The loss of Arctic sea ice has been linked to a variety of atmospheric and oceanic processes, and can be explained by a combination of internal climate variability and anthropogenic forcing (IPCC 2013). As a consequence of a warmer Arctic atmosphere, the summer melt season has become longer, the ocean has absorbed more heat, and the winter freezing has been delayed (e.g., Stroeve et al. 2012b). The recent sea ice loss is also consistent with warmer oceanic conditions in the Barents Sea (Årthun et al. 2012), Fram Strait (Beszczynska-Möller et al. 2012), Bering Strait (Woodgate et al. 2006; Shimada et al. 2006), and the eastern Eurasian basin (Polyakov et al. 2017), as

 Denotes content that is immediately available upon publication as open access.

Corresponding author: Ingrid H. Onarheim, ingrid.onarheim@uib.no



This article is licensed under a Creative Commons Attribution 4.0 license (<http://creativecommons.org/licenses/by/4.0/>).

well as changes in atmosphere, ocean, and sea ice circulation (e.g., Rigor et al. 2002; Lindsay and Zhang 2005; Comiso et al. 2008; Ogi and Wallace 2012; Smedsrud et al. 2017).

Despite a large focus on the changing Arctic sea ice cover, studies tend to be concerned with summer sea ice decline, and with less attention on differences and similarities between seasons and regions. Change and variability in freeze-up over different Arctic regions may be used for winter climate predictions in middle and high northern latitudes (Koenigk et al. 2016), and various regions contribute differently to large-scale atmospheric circulation anomalies (Screen 2017). Enhanced knowledge about regional and seasonal sea ice extent similarities and differences is thus needed.

The Arctic sea ice extent is shrinking in all seasons, but the largest trends are currently found in summer, at the end of the melt season (e.g., Fig. 1; Serreze et al. 2007; Cavalieri and Parkinson 2012). In recent years the reduction in summer sea ice extent has accelerated (Stroeve et al. 2012b); the summer minima have for the last two decades consistently been below the minima inferred from observations beyond the satellite era back to 1850 (Walsh et al. 2017). The largest summer sea ice extent loss has occurred within the Arctic Ocean and is currently largest along the North American and Russian coasts (e.g., Fig. 1b; Comiso et al. 2008; Stroeve et al. 2012b). The loss of sea ice is likely to persist (Kay et al. 2011; Notz and Marotzke 2012; Notz and Stroeve 2016), and a seasonally ice-covered Arctic Ocean is expected by the middle of this century (Notz and Stroeve 2016). The first question this study addresses is the following: How large, and where, is the recent summer sea ice extent loss, and when may regional seas become seasonally ice free?

While the largest observed sea ice changes have occurred in summer and within the Arctic Ocean, sea ice extends well into both the Pacific and Atlantic domains in winter (Fig. 1). The overall decline in winter sea ice extent is smaller than the summer decline, but has increased since the 2000s and is now statistically significant (Meier et al. 2005; Cavalieri and Parkinson 2012). There is, however, to date little loss of winter sea ice extent inside the Arctic basin (Fig. 1c). As the Arctic transits toward an ice-free summer, a further decrease in sea ice extent must increasingly be carried by the winter and first-year ice. The second question we address is the following: How large, and where, is the recent winter sea ice extent loss, and to what extent can an increasing weight carried by the winter be identified at present?

Most studies assessing changes in the Arctic sea ice cover do not go beyond the satellite era. The Arctic sea ice cover displays, however, multidecadal low-frequency

oscillations (Vinje 2001; Polyakov et al. 2003; Divine and Dick 2006), and it expanded for instance in summer from the 1950s to 1980s (e.g., Walsh and Johnson 1979; Mahoney et al. 2008; Gagné et al. 2017), prior to the recent sea ice decline. To evaluate whether the summer and winter contrasts in the satellite era, presented here, are consistent in a longer time frame, we examine the gridded synthesis based on historical observations from 1950 to date provided by Walsh et al. (2015). The overall question we face is the following: What are the regional variations in observed summer and winter sea ice extent loss, and how will they play out in the future?

2. Data and methods

This study concerns the Northern Hemisphere (NH) sea ice cover. To address regional variations, the NH is separated into 13 different regional seas, mostly the Arctic shelf seas and those in the northern Atlantic, North American, and Pacific domains (Fig. 2a). The regional seas and geographical boundaries are consistent with the definitions by the National Snow and Ice Data Center (NSIDC; available online from <ftp://sidacs.colorado.edu/DATASETS/NOAA/G02186/ancillary/>). The Arctic shelf seas are the Beaufort Sea, Chukchi Sea, East Siberian Sea, Laptev Sea, Kara Sea, and Barents Sea. These seas border the polar-most region, the central Arctic. The other regions farther south are the Canadian Archipelago and Hudson Bay (North American domain), Greenland Sea and Baffin Bay/Gulf of St. Lawrence (Atlantic domain), and Bering Sea and Sea of Okhotsk (Pacific domain). We use the term “NH sea ice” when the entire Northern Hemisphere region is assessed. To describe sea ice variability and trends in different seasons, we often exemplify by discussing the sea ice extremes in March (NH sea ice maximum) and September (NH sea ice minimum).

Monthly NH sea ice concentration from 1979 to 2016 is obtained from NSIDC (Cavalieri et al. 1996), derived from the *Nimbus-7* Scanning Multichannel Microwave Radiometer (SMMR), the U.S. Defense Meteorological Satellite Program (DMSP) Special Sensor Microwave Imager (SSM/I), and Special Sensor Microwave Imager/Sounder (SSMIS). The sea ice concentration is gridded to a horizontal resolution of approximately 25 km \times 25 km, on a polar stereographic projection. The NASA Team sea ice algorithm and the method used to derive a consistent dataset are described in Cavalieri et al. (1999) and references therein.

To examine the NH sea ice cover before the satellite era, we use the NSIDC gridded monthly sea ice extent and concentration, 1850 onward, version 1 dataset (hereinafter referred to as the Walsh data; Walsh et al.

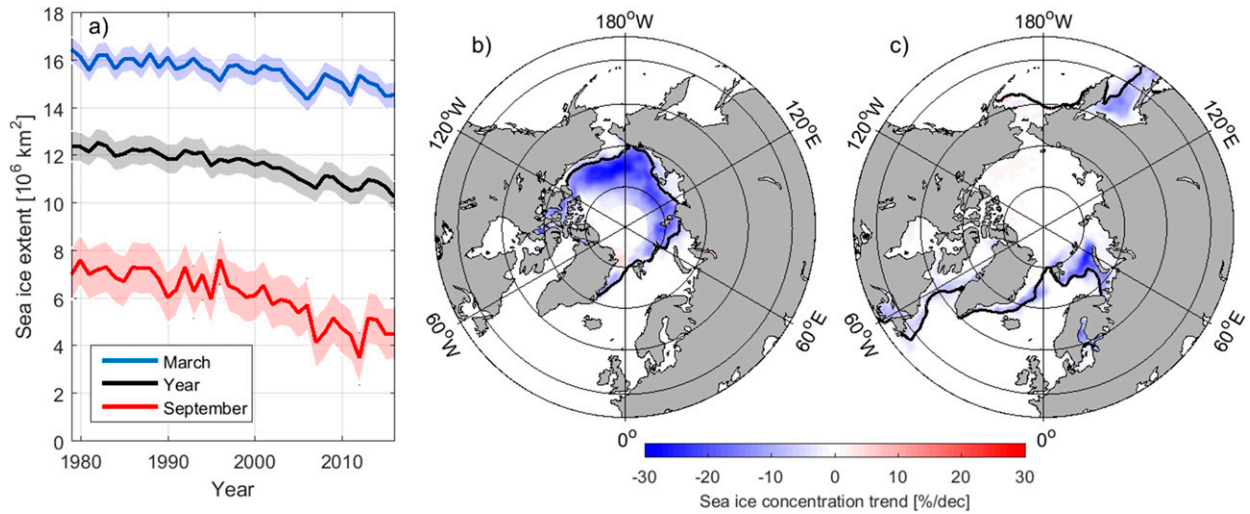


FIG. 1. (a) March (blue), September (red), and annual mean (black) Northern Hemisphere sea ice extent, 1979–2016. Shaded regions indicate plus and minus one standard deviation. Linear sea ice concentration trends ($\% \text{dec}^{-1}$) in (b) September and (c) March, 1979–2016. Black contours show the mean sea ice edge.

2015, 2017), providing gridded (0.25° latitude \times 0.25° longitude) midmonth sea ice concentrations from 1850 to 2013. The Walsh data build on the commonly used dataset by Chapman and Walsh (1991a, b; cf. e.g., Maslanik et al. 1999; Titchner and Rayner 2014), but add additional historical sources, extend the time series, and refine the merging of the data sources. In total, 16 different data sources contribute to the dataset, including historical ship observations, compilations by naval

oceanographers, and national ice services. Satellite passive microwave data, calculated by combining output from the bootstrap and NASA Team algorithms (Meier et al. 2013), constitute the data coverage since 1979. It thus constitutes the longest NH sea ice concentration record based on observations.

We use the historical dataset as provided, but restrict our analysis to the relatively well-observed period onward from 1950 as documented below. Detailed

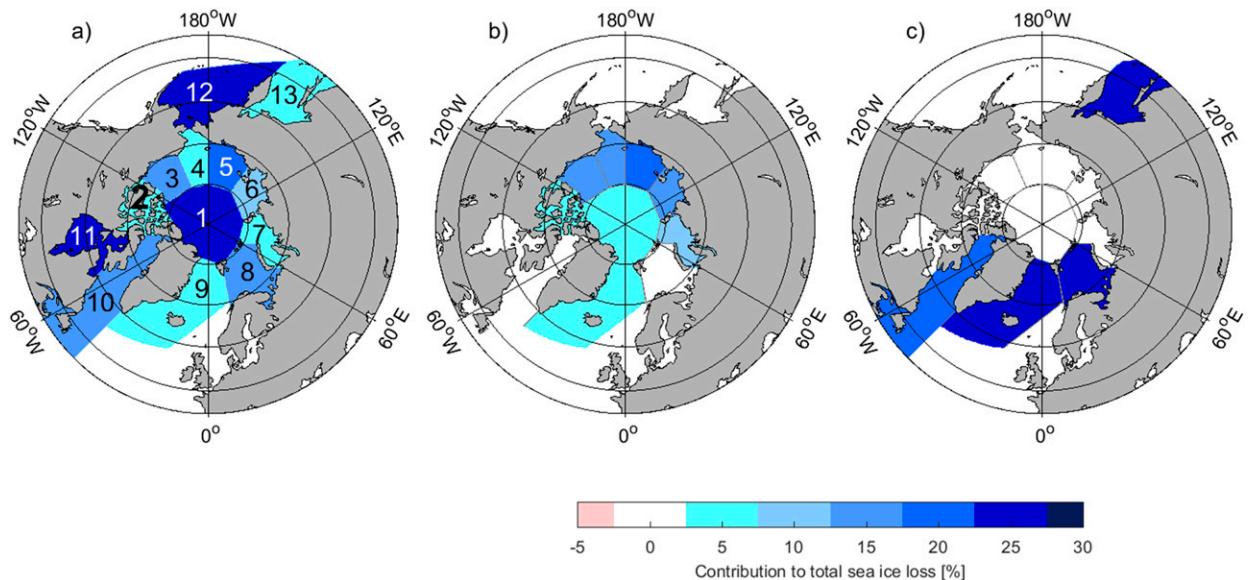


FIG. 2. (a) The Northern Hemisphere regional seas, clockwise from 90°N : 1) central Arctic, 2) Canadian Archipelago, 3) Beaufort Sea, 4) Chukchi Sea, 5) East Siberian Sea, 6) Laptev Sea, 7) Kara Sea, 8) Barents Sea, 9) Greenland Sea, 10) Baffin Bay/Gulf of St. Lawrence, 11) Hudson Bay, 12) Bering Sea, and 13) Sea of Okhotsk. Contribution from each regional sea to the (b) September and (c) March Northern Hemisphere sea ice extent trends, 1979–2016.

uncertainty estimates are unfortunately not provided with the dataset, presumably from the synthesis of multiple sources required to produce a hemisphere-scale gridded dataset. [Gagné et al. \(2017\)](#) for instance find that the Walsh data in the eastern Arctic are associated with less variance and trends than the Russian Arctic and Antarctic Research Institute (AARI) sea ice concentration dataset since 1950. The Walsh data should therefore be approached with this caveat in mind.

However, [Walsh et al. \(2015\)](#) do detail the temporal and regional coverage of the different data sources in their synthesis. The data coverage can be summarized as follows. The Arctic-wide data record is essentially continuous since 1953 ([Walsh and Johnson 1979](#)). The presatellite data availability is typically larger in summer than winter, and there is direct observational coverage in practically all regions in all years in both summer and winter. In the Arctic shelf seas, the observations of the Russian AARI contribute 40%–90% data coverage. On the hemisphere-scale, the analog Walsh and Johnson ice concentration data contribute the largest coverage in March and September (typically 60%–80%). The AARI database is the second largest contributor to general NH data coverage in these months (typically 10%–20%) for 1950–78. The Walsh data also include observations from, for example, Naval Oceanographic Office sea ice maps (mainly in the North American, Atlantic, and Pacific domains; typically less than 20%), Arctic Climate System Study data (Atlantic domain; 10%–80%), and Japan Meteorological Agency charts (sporadically up to 30% in the Pacific domain). Analog filling added by [Walsh et al. \(2015\)](#) amounts to less than 10% of the data. We refer the reader to [Walsh et al. \(2017\)](#), and references therein, for further details.

In addition to restricting our use of the historical data in time, we furthermore consider sea ice extent rather than sea ice area or concentration; most historical observations are of the sea ice edge, and hence most directly represent extent. Sea ice extent is beneficial also in the satellite era because sea ice concentration derived from passive microwaves can be biased during melt ([Cavalieri et al. 1992](#)). Sea ice extent is calculated as the cumulative area of all grid cells having at least 15% sea ice concentration. In the northernmost region sea ice extent is furthermore beneficial over concentration or area as observations are lacking near the pole throughout the satellite record. We assume the unobserved area to be at least 15% ice covered. Normalized sea ice extent is the regional monthly sea ice extent divided by the regional maximum sea ice extent (for 8 out of 13 regions, this is the full domain). We note that when considering the Walsh data we do not go beyond 2013, as merging of the bootstrap and NASA Team product, and the NASA

Team product causes inconsistency in the time series in some regions (not shown).

Correlation r and variance explained r^2 are calculated for detrended time series, unless otherwise stated. The F statistics are used to test the significance of linear trends, with no trend as the null hypothesis. Statistical significance is associated with a 95% confidence level. Linear trends are calculated using the least squares approach.

3. Recent Northern Hemisphere sea ice variability and trends (1979–2016)

The annual mean NH sea ice extent has decreased by 2.0×10^6 km² since 1979 ([Fig. 1a](#)). The sea ice extent loss is significant throughout the year ([Table 1](#); [Cavalieri and Parkinson 2012](#)), and with the largest changes occurring in summer in agreement with previous studies (see also, e.g., [Cavalieri and Parkinson 2012](#); [Serreze et al. 2007](#)). Updated through 2016, the sea ice extent has decreased by 45% in September, 35% in August, and 26% in July, relative to 1979. The smallest changes, still significant, occurred in winter and early spring and are close to 9% in March, April, and May.

The NH sea ice extent changes are, however, characterized by large regional variations. The summer sea ice extent loss is widespread throughout the Arctic Ocean ([Fig. 1b](#); [Stroeve et al. 2012b](#)) with largest trends along the North American and Russian coasts, whereas the winter loss generally occurs farther south ([Fig. 1c](#) and [Table 1](#)). Although the overall NH sea ice extent decline is twice as large in September as in March, regional winter trends (e.g., in the Barents Sea) are equal to the largest summer trends of other regions. The Bering Sea has positive trends throughout the winter ([Table 1](#)). To further assess seasonal and regional differences in NH sea ice variability and change, we first examine trends in September and March. We note that there may be regional differences within the regional seas assessed here; however, our qualitative results do not appear fundamentally concerned with the specific choice of regions. For a more detailed description of timing and geographical distribution of onset of rapid sea ice decline, the reader is referred to [Close et al. \(2015\)](#).

The September NH sea ice extent has decreased by 3.2×10^6 km² since 1979, in which the East Siberian Sea (contributing with 22%), Chukchi Sea (17%), Beaufort Sea (16%), Laptev Sea (14%), and Kara Sea (9%) contribute the most ([Table 1](#) and [Fig. 2b](#)). These regions typically have large interannual summer variability and trends, but they are fully ice covered in winter ([Figs. 3](#) and [4](#)). Combined, these five perennial ice-covered seas account for 89% of the interannual variance in the NH September sea ice extent since 1979 (not shown). The

TABLE 1. Regional monthly sea ice extent loss (10^4 km^2) for 1979–2016. The three largest monthly contributors to the Northern Hemisphere sea ice loss are in italic. Boldface values indicate trends that are statistically significant.

| Month | Central Arctic | | | East Siberian | | | | | NH | | | |
|-------|----------------|--------------|--------------|---------------|--------------|--------------|--------------|--------------|--------------|--------------|-------------|--------------|
| | Canadian | Beaufort | Chukchi | Siberian | Laptev | Kara | Barents | Greenland | | Baffin | Hudson | Bering |
| Jan | -3.7 | 0.0 | 0.0 | 0.0 | 0.0 | -1.2 | -49.2 | -35.3 | -47.5 | -0.3 | 6.2 | -40.9 |
| Feb | -3.2 | 0.0 | 0.0 | 0.0 | 0.0 | -2.1 | -46.5 | -36.4 | -46.1 | 0.0 | 5.3 | -38.2 |
| Mar | -1.9 | 0.0 | 0.0 | 0.0 | 0.0 | -0.4 | -41.4 | -34.9 | -33.8 | 0.0 | 1.7 | -40.8 |
| Apr | -0.4 | 0.0 | 0.0 | 0.0 | 0.0 | -0.2 | -47.8 | -26.5 | -24.4 | 0.0 | 10.7 | -46.1 |
| May | -0.9 | -0.2 | -0.3 | 0.0 | -0.2 | -0.6 | -58.8 | -18.2 | -23.3 | -1.1 | 3.0 | -15.2 |
| Jun | -1.8 | -1.8 | -9.5 | 0.6 | -4.6 | -14.7 | -59.6 | -15.8 | -29.7 | -18.4 | -2.6 | -3.7 |
| Jul | -5.3 | -4.9 | -18.0 | -6.5 | -22.5 | -53.3 | -34.2 | -18.8 | -40.1 | -51.3 | -0.5 | 0.0 |
| Aug | -10.7 | -18.8 | -38.4 | -50.2 | -35.7 | -41.9 | -9.8 | -14.8 | -11.9 | -10.8 | 0.0 | 0.0 |
| Sep | -21.9 | -22.7 | -48.9 | -70.7 | -44.6 | -28.8 | -5.8 | -12.6 | -2.7 | -3.6 | -0.6 | 0.0 |
| Oct | -8.1 | -8.8 | -41.2 | -33.6 | -10.0 | -42.0 | -23.0 | -10.1 | -24.3 | -11.0 | -1.2 | -0.1 |
| Nov | -4.7 | -0.2 | -23.5 | -0.8 | 0.0 | -26.6 | -41.9 | -17.0 | -24.5 | -58.1 | -7.8 | -2.3 |
| Dec | -3.4 | 0.0 | 0.0 | 0.0 | 0.0 | -8.6 | -51.7 | -28.0 | -29.9 | -6.0 | -9.3 | -14.5 |

recent large summer sea ice extent loss has resulted in very little sea ice being left in September in the Chukchi, East Siberian, Laptev, and Kara Seas. The central Arctic and Canadian Archipelago together contribute to 14% of the NH September loss.

The seasonally ice-covered seas farther south dominate NH winter variability and change (Figs. 3 and 4). The largest contributors to the NH March sea ice extent loss ($1.5 \times 10^6 \text{ km}^2$ since 1979) are the Barents Sea (27%), Sea of Okhotsk (27%), Greenland Sea (23%), and Baffin Bay/Gulf of St. Lawrence (22%) (Table 1 and Fig. 2c). The four seas also account for 81% of the interannual variance in the NH March sea ice extent since 1979 (not shown). These regions are practically ice free in summer (Fig. 3).

Within the Arctic Ocean (i.e., the Beaufort, Chukchi, East Siberian, Laptev, Kara, and Barents Seas and the central Arctic) the winter sea ice extent variability and loss have almost exclusively occurred in the Barents Sea (Table 1). The other regions are essentially fully ice covered in winter, neither contributing to interannual variability nor trends. The Barents Sea has contributed to 95% of the observed March sea ice extent loss in the Arctic Ocean since 1979, and also carried the interannual variability in Arctic Ocean sea ice extent ($r^2 = 0.99$, standard deviations are 0.17×10^6 and $0.18 \times 10^6 \text{ km}^2$ in the Barents Sea and Arctic Ocean, respectively). The Barents Sea has thus carried the variability and trend in the winter Arctic Ocean sea ice extent to date (Onarheim et al. 2015), and will continue to do so until other Arctic seas may get open-water areas in winter in the future.

4. Long-term Northern Hemisphere sea ice variability (1950–2013)

The NH sea ice extent displays pronounced interannual variability both in summer and winter over the longer time period since 1950 (Fig. 5; Walsh et al. 2017). The sea ice extent increases slightly in the 1950–70s, particularly in summer, and is followed by the rapid sea ice loss in recent years (Fig. 5a), consistent with findings by, for example, Polyakov et al. (2003), Mahoney et al. (2008), and Gagné et al. (2017). The 15 smallest annual mean NH sea ice extents since 1950, updated through 2016, all appear during the last 15 years, with the 10 smallest extents within the 12 last years. Both interannual and multidecadal variations in the Walsh data are more prominent in summer than winter, but are associated with large regional differences (Fig. 5; Walsh et al. 2017).

To examine long-term sea ice extent changes regionally, we first contrast the time periods 1950–99 and 2000–13, as the largest sea ice extent minima occurred

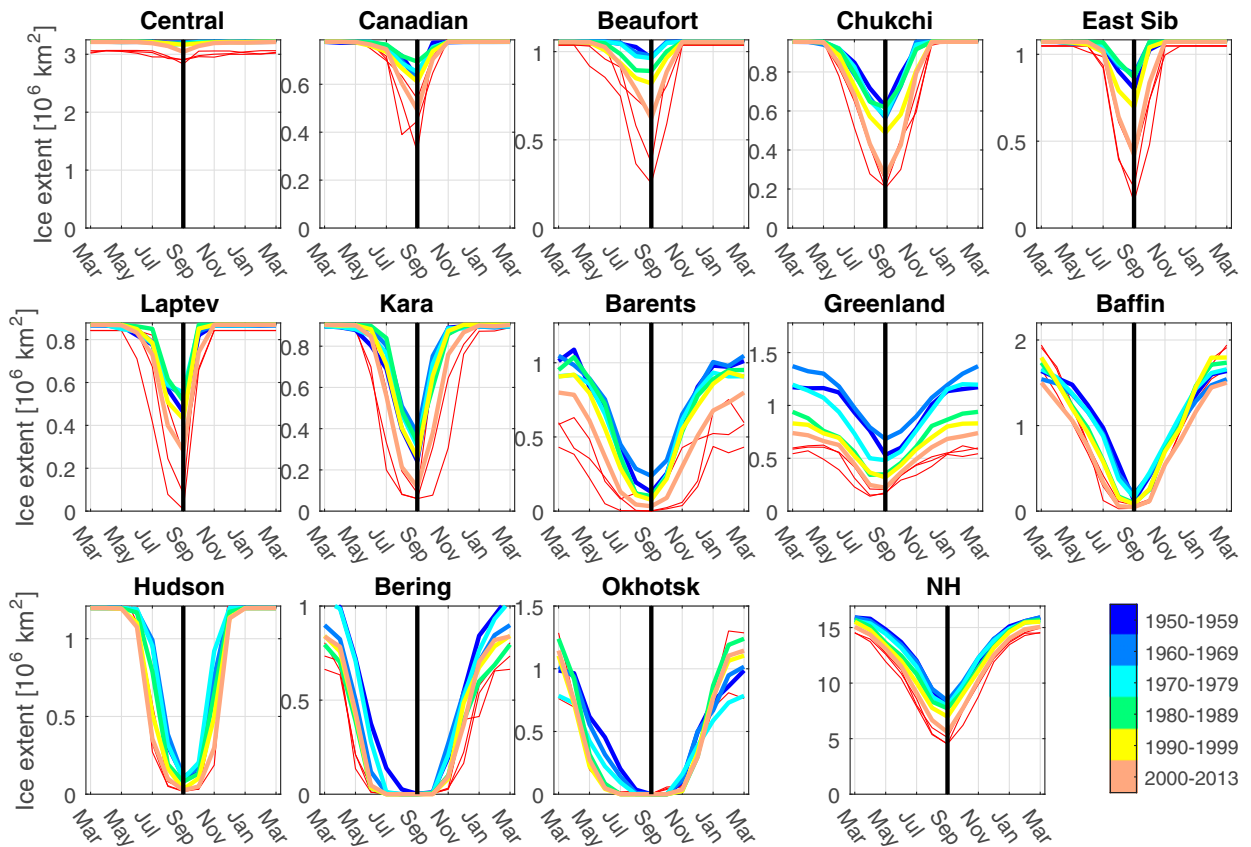


FIG. 3. Monthly sea ice extent for the Northern Hemisphere and its individual seas in successive 10-yr periods from 1950 to 2013 (Walsh et al. 2015). The seasonal cycles are shown from March to March, centered around September. Months before (to the left) of September represent the melt season, whereas months after (to the right) of September represent the freezing season. The three thin red lines indicate the sea ice extent in 2014–16 (Cavalieri et al. 1996).

after year 2000 (Fig. 5a). Summer and winter variability is exemplified by assessing sea ice variability in September and March. Figure 5b shows a September sea ice cover that is generally within the Arctic Ocean throughout the 1950–2013 time period, but with a present poleward contraction of the sea ice edge. The Arctic Ocean is mainly completely ice covered throughout the 1950–99 period, except for parts of the Barents, Kara, and Laptev Seas (Fig. 5b). The NH September sea ice extent loss since 1950 has thus predominantly occurred in the satellite era (Fig. 5a; Mahoney et al. 2008).

The March sea ice edge generally extends beyond the Arctic Ocean, with the Barents Sea as the prominent exception (Fig. 5c). The recent poleward shift of the March sea ice edge is generally smaller than the September change. In the Greenland and Barents Seas, however, the winter sea ice edge is distinctly farther north in recent years compared to in the 1950–99 period (Fig. 5c). Divine and Dick (2006) have suggested that recent sea ice retreat in the Greenland and Barents Seas may be part of a multidecadal oscillation, superimposed

on a long-term sea ice retreat since the second half of the nineteenth century (Vinje 2001).

It was shown that the Beaufort, Chukchi, East Siberian, Laptev, and Kara Seas carry the recent NH September sea ice extent loss (e.g., Fig. 2b). These regions also account for 88% of the interannual variance in NH September sea ice extent between 1950 and 2013 (Fig. 6a). The Greenland and Barents Seas largely account for the remaining variability, and contribute to the multidecadal variability (not shown). We note that these conclusions are drawn from an incomplete observational basis; however, most of the Arctic shelf seas have 40%–90% data coverage in sea ice concentration in September (not shown), and we only consider sea ice extent.

The NH March sea ice extent variability and trends are explained by sea ice changes in the Barents Sea, Greenland Sea, Baffin Bay/Gulf of St. Lawrence, and Sea of Okhotsk, and these seas carry 86% of the interannual NH March sea ice extent variability throughout the observational record (Fig. 6b). The winter sea ice cover in the Barents Sea, Greenland Sea, and Baffin

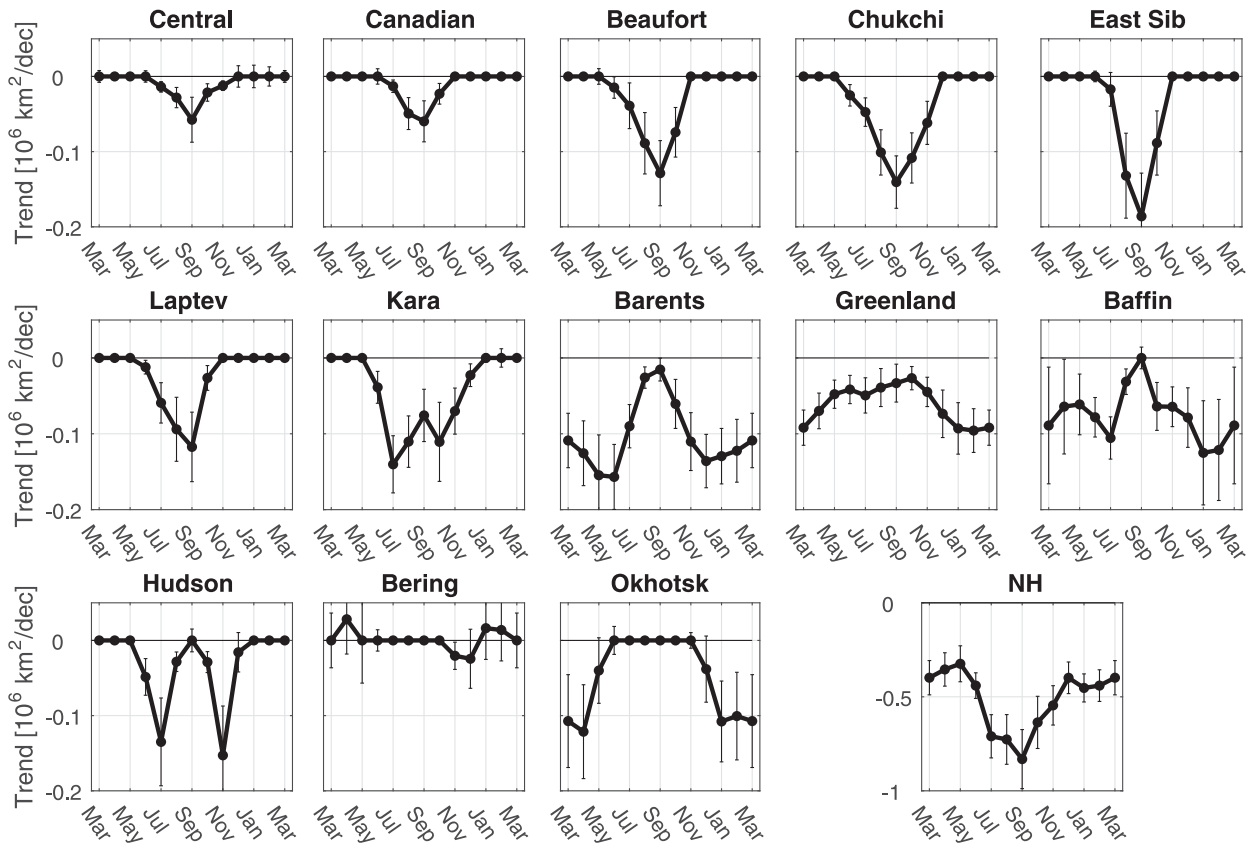


FIG. 4. Monthly trends in sea ice extent for the Northern Hemisphere and its individual seas, 1979–2016. The trends are shown from March to March, centered around September. Months before (to the left) of September represent the melt season, whereas months after (to the right) of September represent the freezing season. Bars indicate 95% confidence intervals.

Bay/Gulf of St. Lawrence is relatively well observed since the 1950s (typically 20%–80% observational data coverage prior to 1979; not shown), whereas the Sea of Okhotsk is in general sparsely observed before the satellite era. We find from the Walsh data that the distinct spatial differences between the NH September and March sea ice extent variability (i.e., summer variability in the north and winter variability generally farther south) appear consistent over 60 years in the observation-based data (Figs. 5 and 6).

5. Summer, winter, and transition modes

Recent NH sea ice extent appears unprecedentedly small both in summer and winter based on the available observations (Figs. 1 and 5; Walsh et al. 2017). The overall NH trends for 1979–2016 (Fig. 4) are statistically significant in all months and approximately twice as large in summer as in winter (Table 1). The matrixed data of Fig. 7 offers a concise summary of the monthly and regional sea ice extent trends since 1979. The most poleward regions are characterized by loss restricted to a

few summer months and most strongly so in September; this may be unsurprising, but only to the extent that a perennial sea ice cover remains. These northern regions have their largest sea ice extent variability and trend in summer (Fig. 3), and are therefore hereafter described as being in a “summer mode.” The regions in summer mode at present are the central Arctic, Canadian Archipelago, the Beaufort, Chukchi, East Siberian, Laptev, and Kara Seas, and Hudson Bay. Moving clockwise and southward (toward the right in Fig. 7), the extent of change tends to broaden from summer toward winter, eventually to the extreme that summer sea ice is practically absent, a seasonal ice cover is realized, and change is more pronounced in winter.

The regions with largest sea ice extent variability and trend in winter are hereafter referred to as being in a “winter mode.” The regions in winter mode at present are generally the seas outside the Arctic Ocean, but importantly also the Barents Sea (cf. Fig. 7; Figs. 1c and 5c); that is, it characterizes the Barents Sea, Greenland Sea, Baffin Bay/Gulf of St. Lawrence, Bering Sea, and Sea of Okhotsk. Where the summer and winter modes

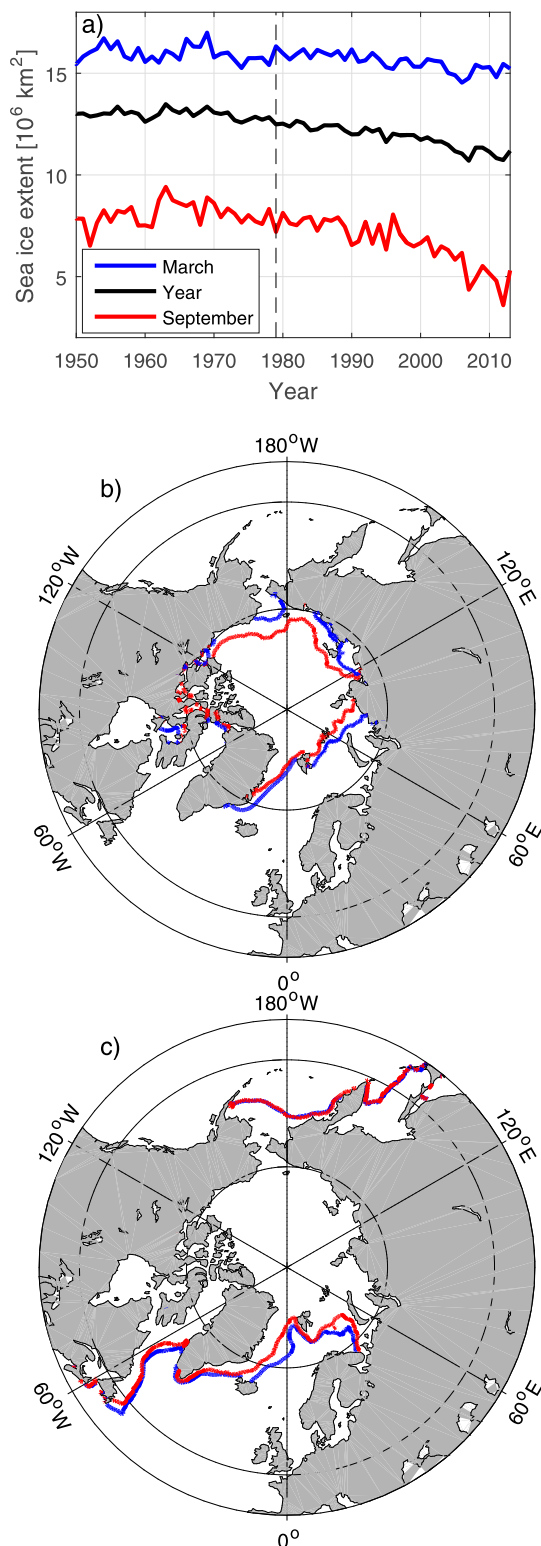


FIG. 5. (a) Northern Hemisphere sea ice extent, 1950–2013 (Walsh et al. 2015), for September (red), March (blue), and the annual mean (black). The vertical dashed line indicates 1979. The mean (b) September and (c) March sea ice edge for the 1950–99 (blue) and 2000–13 periods (red).

spatially connect, a “transition mode” can be associated. The Kara, Barents, and Greenland Seas and Hudson Bay could thus also be placed in the transition mode (cf. Figs. 1b and 5b and Figs. 1c and 5c). The transition mode is characterized by sea ice extent variability and change in both summer and winter (similar to the Greenland Sea in Fig. 3), or largest variability and change in spring and fall (similar to Hudson Bay in Fig. 3). The NH sea ice cover as a whole is in transition mode, with large variability and trends in both summer and winter (Figs. 3 and 4).

The summer mode regions are typically completely ice covered in winter, whereas winter mode regions are typically ice free in summer. The transformation from summer to winter mode thus implies a substantial change in the regional sea’s seasonal cycle; from a perennial to a seasonal sea ice cover. The gradual transformation between the different modes suggests that regions may change from one mode to another in the future, or that they may have done so in the past. Implicit to the summer mode’s larger retreat in summer than winter is an increasing range of the seasonal cycle, and the seasonality, calculated as the difference between the annual sea ice extent maximum and minimum divided by the annual mean, increases in all summer mode regions. The largest amplification of the seasonal cycle has occurred in the East Siberian Sea (Fig. 3). The winter mode regions experience, in contrast, decreased range of the seasonal cycle, by going toward ice-free conditions year-round.

a. Past variability in modes

Here we examine whether some regions may have transformed from one mode to another according to the observation-based record back to 1950. By assessing monthly mean sea ice extent between 1950 and 2013, we find that the Barents Sea and Baffin Bay/Gulf of St. Lawrence used to have a partial summer sea ice cover until the recent decades, whereas they are presently in winter mode and essentially ice free in summer (Fig. 3). These seas have thus completed the transition mode, with sea ice variability and trends in both summer and winter, and entered the winter mode, with only winter variability and trends.

The remaining seas we find have remained in the same mode since 1950 according to the Walsh data. We note, however, that the Kara Sea and Hudson Bay are currently becoming ice free in summer, and thus entering transition mode. Section 7 assesses possible future transformations between modes in a climate that continues to warm.

b. Present state

The NH sea ice extent decline is currently largest in summer (e.g., Fig. 4; Serreze et al. 2007). Figure 8 illustrates the observed regional change in September and March between 1950 and 2013. Again going clockwise

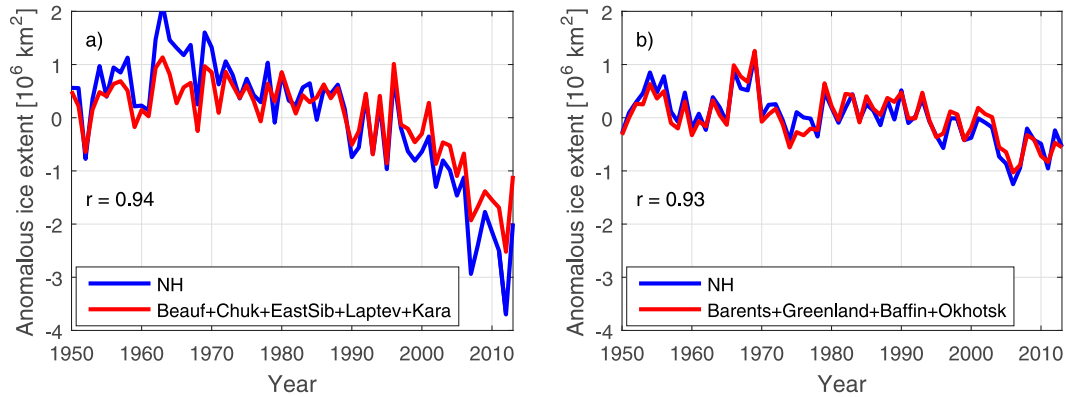


FIG. 6. Anomalous Northern Hemisphere sea ice extent (blue) in (a) September and (b) March, 1950–2013 (Walsh et al. 2015). Anomalous sea ice extent (red) in the Beaufort, Chukchi, East Siberian, Laptev, and Kara Seas in (a) (summer mode regions) and Barents Sea, Greenland Sea, Baffin Bay/Gulf of St. Lawrence, and Sea of Okhotsk in (b) (winter mode regions).

and southward from the central Arctic (toward the right in Fig. 8; same order as in Fig. 7), regions typically become gradually less ice covered (they get smaller normalized extent), and summer and winter trends (length of vertical arrows) decrease and increase, respectively.

As regions become ice free in summer (reach the hatched area in Fig. 8), they enter transition mode.

Figure 8 summarizes how the summer mode regions have large changes in the minimum sea ice extent (Fig. 8, top), and how winter change dominates in the winter

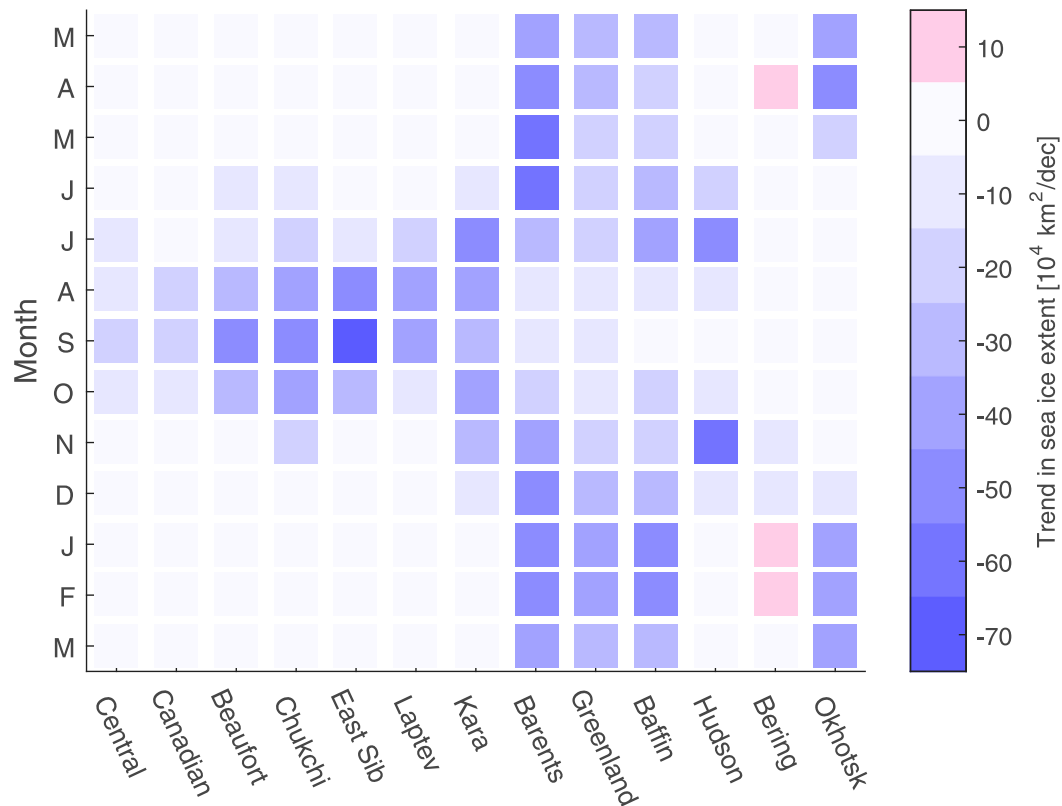


FIG. 7. Monthly trends in sea ice extent for the Northern Hemisphere regional seas, 1979–2016. The regions are ordered from left to right along the x axis in a clockwise direction through the Arctic Ocean from the central Arctic in the north and southward to the Atlantic, North American, and Pacific domains (i.e., against the main Atlantic water flow in the Arctic Ocean). On the y axis, months are ordered from March to March, and centered around September.

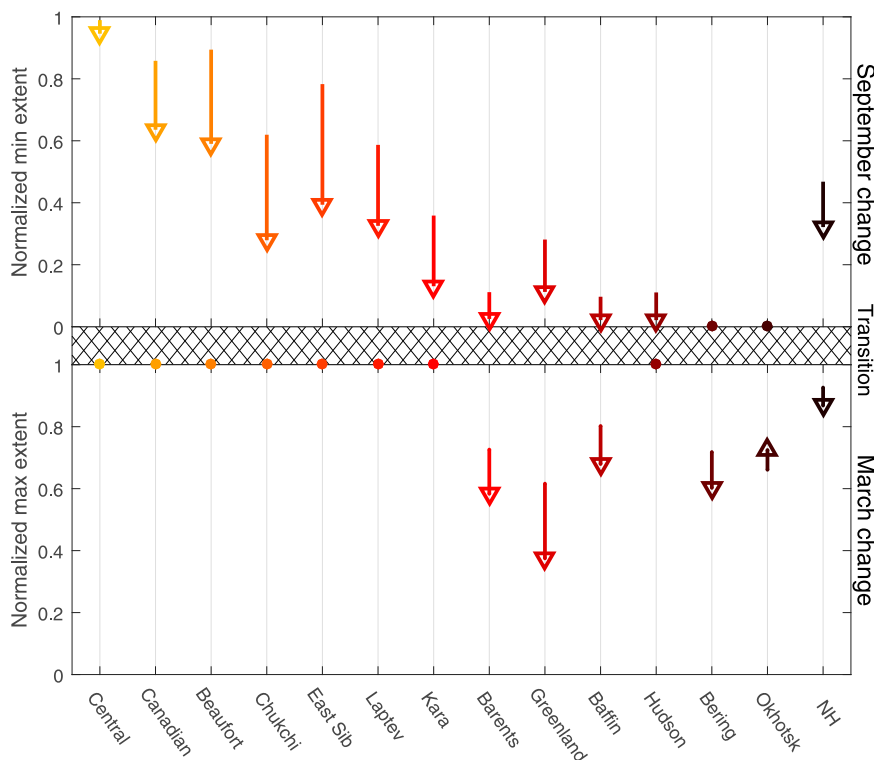


FIG. 8. Regionally normalized sea ice extent change in (top) September and (bottom) March. Arrows represent regional change in sea ice extent between the 1950–99 mean (arrow tail) and the 2000–13 mean (arrowhead). Dots indicate no change in regional max and min sea ice extent between the two periods. A normalized extent of 1 (0) indicates complete (no) sea ice cover. The hatched area illustrates the transition mode between summer and winter variability; that is, a region reaching no summer sea ice [0 in (top)] enters the transition mode (hatched region); when the ice cover starts to decrease in winter, the region enters winter mode at (bottom).

mode regions (Fig. 8, bottom). The summer sea ice extent has also decreased in most winter mode regions since the 1950s, and summers are now ice free, except for the Greenland Sea. Overall, there is an approximate 2:1 ratio for September versus March trend for the Northern Hemisphere sea ice extent loss (cf. also NH in Fig. 4).

We note that the linear trend in Bering Sea winter sea ice extent is positive since 1979 (Table 1), but negative when considering the longer time frame since 1950 (Fig. 8). The recent positive trend may be linked to internal variability (Gagné et al. 2017). The slightly increasing winter sea ice extent estimated for the Sea of Okhotsk since the 1950s may be influenced by the regional sparsity of winter observations before the 1970s (not shown; Walsh et al. 2017), and is contrasted by the rapid decline since 1979 (e.g., Fig. 4).

6. Seasonal asymmetry in summer and winter modes

We identified the current summer and winter mode regions based on their sea ice extent variability and trends in summer versus winter since 1979 (e.g., Fig. 7).

At present, there are also other fundamental differences between the two modes; we find seasonal asymmetry in extent and trends comparing the melt and freezing seasons, particularly for the present summer mode regions (Figs. 3 and 4; the melt season is considered to be the months between the sea ice extent maximum in March and the minimum in September, and similarly the months between September and March define the freezing season). The seasonal cycle of the NH sea ice extent as a whole broadly follows a sinusoidal (Fig. 3), but with the largest monthly trends in September and the smallest in May (Fig. 4) (i.e., the trends are not symmetric around September). The sea ice loss is predominantly carried by the months July, August, and September, and the NH loss is thus slightly larger in the melt season compared to the freezing season (Fig. 4).

The individual present summer mode regions also have larger trends in the months prior to the late melt season than in the early freezing season (Fig. 4). In, for example, the Laptev Sea, there is retreat from June to October, with the trend being larger in August and July than in June and October. The Laptev Sea is fully ice

covered within two months after the September sea ice extent minimum, and has thereby no trend in November (Fig. 4). The asymmetry with larger trends in the melt season compared to the freezing season, demonstrates that sea ice melt is enhanced in spring and that melt occurs earlier, but that the sea ice cover refreezes rapidly after the sea ice extent minimum in September. The ocean typically refreezes completely within two months after the sea ice extent minimum in the central Arctic, Canadian Archipelago, Beaufort Sea, East Siberian Sea, and Laptev Sea, whereas it refreezes by December in the Chukchi Sea, and by January in the Kara Sea (Fig. 3).

In contrast to the summer mode, seasonal trends in the winter mode regions are essentially symmetric (Fig. 4). Large trends in fall indicate that the freeze-up is reduced or delayed, and that open-water areas persist further into winter (Fig. 3). Negative trends in the melt season indicate that sea ice melt is enhanced in spring.

The current asymmetry (symmetry) in the summer (winter) mode regions is not implicit to the proposed modes, and may be due to regional settings. We note that the present summer mode regions are tightly linked regionally, whereas the winter mode regions are generally more disconnected, largely separated by continents and with the summer mode Arctic Ocean between the Atlantic and Pacific sectors. The regional climatic forcing can thus differ substantially (e.g., Cavalieri and Parkinson 1987; Smedsrud et al. 2013).

As areas of open water develop earlier in the melt season, the upper ocean absorbs more solar radiation, basal and lateral sea ice melt increase, and the ocean absorbs more heat (e.g., Perovich et al. 2007). Large negative sea ice extent trends in the melt season, particularly in the summer mode regions (Fig. 4), thus appear accelerated by the ice–albedo feedback (Stroeve et al. 2014) (i.e., caused by more melting). We note that parts of the large open-water regions in the Arctic shelf seas may also be due to sea ice divergence along the coasts, a more mobile sea ice cover (Rampal et al. 2009), and above-normal sea ice export in Fram Strait (Williams et al. 2016; Smedsrud et al. 2017).

Despite decreasing summer sea ice extent minima and a warmer ocean at the end of the melt season (Steele and Dickinson 2016), the summer mode regions still refreeze rapidly in fall and reach a complete sea ice cover (Fig. 3). The rapid refreeze indicates that the ocean efficiently loses its heat to the atmosphere in fall.

One way to evaluate the freeze-up is to estimate how quickly new ice forms. We estimate the tendency for large areas to freeze-up by quantifying rapid ice growth events (RIGEs; Fig. 9), defined here as an increase in sea ice extent of at least 10^6 km^2 over a weeklong period. We find that RIGEs primarily occur during the month of

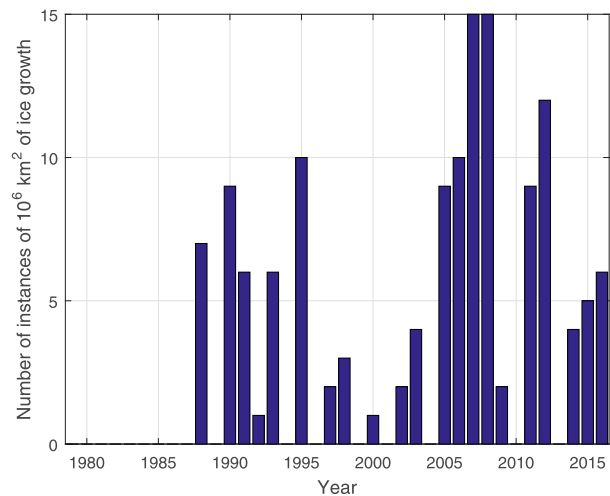


FIG. 9. Number of yearly RIGEs, that is, an increase in sea ice extent of at least 10^6 km^2 over a weeklong period, 1979–2016. The RIGEs are computed as a weekly running mean, so the number of occurrences can imply either a consecutive number of weeklong periods where at least 10^6 km^2 of sea ice form in a row, or it can also occur at different times during winter. Note that there were no RIGEs between 1979 and 1987.

October (although they may also occur as late as December; not shown). All the RIGEs are observed in the Arctic Ocean within the current summer mode regions (not shown). As seen in Fig. 9, the number of RIGEs has increased in recent decades following record minima in Arctic sea ice extent. For example, in 2007 and 2008 there were 15 consecutive 7-day periods in October through early November where more than 10^6 km^2 of sea ice formed. Similarly, in 2012, the lowest September minima recorded to date, the 12 RIGEs all occurred in October. The summer mode regions' small trends in the freezing season can thus be related to the increasing number of RIGEs.

The increasing number of RIGEs in the summer mode regions may be related to the summer mode regions' strong salinity stratification. The Arctic shelves receive strong river runoff in summer (Rudels 2015; Rawlins et al. 2010), and the consequent strong stratification suggests that the increased amount of heat absorbed by the ocean in summer generally accumulates in the upper ocean. When the ocean surface cools in fall, and thereby densifies, the strong salinity stratification limits vertical displacements, and thereby inhibits warmer waters to be brought up from below. Consequently, only the upper layer has to cool to the freezing point before sea ice formation starts. Sea ice generally forms quickly within the Arctic Ocean once temperatures drop below freezing (Stroeve et al. 2014).

In contrast to the summer mode, the winter mode regions experience large trends of sea ice retreat also in

the months following the annual sea ice extent minimum (Fig. 4), with delayed and more gradual freeze-up in fall (Fig. 3). Consistently, no RIGEs are observed to compensate for decreasing sea ice extent in the winter mode regions. The winter mode regions are more climatologically heterogeneous and more geographically separated. The regional conditions appear generally less favorable for RIGEs than in the Arctic proper, as alluded to below.

Changes in the Atlantic domain exert a dominant role on winter sea ice loss in the Barents Sea (Årthun et al. 2012), Nansen basin (Onarheim et al. 2014), and the eastern Eurasian basin (Polyakov et al. 2017). The Atlantic heat inhibits sea ice freezing (Årthun et al. 2012), and maintains a warmer less stratified water column inhibiting RIGEs in the freezing season.

Moving westward, Arctic sea ice is generally advected to and through the Greenland Sea (Kwok 2009), where there up to the 1980s also used to be local sea ice formation in the so-called Odden ice tongue (Wadhams and Comiso 1999; Comiso et al. 2001). The Norwegian Atlantic Current inhibits local sea ice formation and keeps the eastern parts of the Greenland Sea ice free year-round. The current, by lateral mixing, also provides the heat given up through open-ocean convection in the central basin thus maintaining a weakly stratified water column (Rudels et al. 1989; Dickson et al. 1996) and scarce sea ice formation. Variations in the Greenland Sea ice cover are, however, largely atmospherically driven (Fang and Wallace 1994; Deser et al. 2000).

Also the Baffin Bay/Gulf of St. Lawrence receives sea ice exported from the Arctic Ocean (Kwok 2005). Sea ice also forms locally (e.g., Close et al. 2018), and the sea ice variability depends largely on atmospheric conditions including the North Atlantic Oscillation (NAO; Fang and Wallace 1994; Deser et al. 2000). We note that this region extends far southward into the North Atlantic Ocean with generally higher air temperatures and solar radiation providing heat throughout the year.

The Bering Sea and Sea of Okhotsk are also relatively southern, both being south of the Arctic Circle, and particularly the Sea of Okhotsk is practically disconnected from the Arctic Ocean (cf. Fig. 2). Both regions have atmospherically driven sea ice formation in the north, and the ice melts when it drifts southward into warmer water (Muench and Ahlnas 1976; Martin et al. 1998; Kimura and Wakatsuchi 1999). Whereas the Bering Sea is more characterized by variance than trends, the latter partly positive (Fig. 4), there is reduced sea ice formation in the Sea of Okhotsk in fall linked to increasing air temperatures (Kashiwase et al. 2014).

We have demonstrated that the northernmost (summer mode) regions currently refreeze rapidly in fall,

contrasting the regions farther south (winter mode). Although actual drivers of regional and seasonal sea ice distribution are not extensively assessed herein, we submit from the above that asymmetry between the melt and freezing seasons—and summer and winter modes—reflects a region's climatological preconditioning, and more specifically that the combination of a freezing polar night and freshwater stratification sustains RIGEs in the present summer mode regions.

7. Future perspectives

If the Northern Hemisphere sea ice loss persists, the Arctic Ocean will become seasonally ice free, and further reduction of sea ice extent will have to be increasingly concerned with wintertime change. Summer mode regions will accordingly shift via transition mode into winter mode. A winter mode region can in this perspective be understood to be at a later stage in the transformation from a complete sea ice cover to ice-free conditions, than a summer mode region.

a. Space for time?

Different seas are at different stages—the modes—as part of one overall transformation in time (i.e., the general 2:1 ratio of September vs March retreat of total NH sea ice extent; cf. Figs. 4 and 8). A geographical region's transformation in time from a complete perennial sea ice cover to none (i.e., sequentially going through the summer, transition, and winter modes) implies that Fig. 7 offers a possible “space for time” perspective on the evolution of Arctic sea ice extent as current change moves poleward. Figure 7 then represents, looking right, a regional sea's further sequence of change moving forward in time.

Keeping in mind the more disconnected nature of the Pacific regional seas (cf. section 6), the above concept is probably most relevant from an Atlantic perspective (cf. also the general spatial trend patterns in Figs. 7 and 8). We further note that the regional ordering of Figs. 7 and 8 from the central Arctic (summer mode) and clockwise along the Arctic shelf seas toward the Atlantic domain farther south (winter mode), is generally against the poleward flow of Atlantic water. The closer to the inflow of Atlantic water, the generally larger winter trends and smaller summer trends. The Barents and Kara Seas are accordingly at the cusp of recent and present Arctic transformation from summer to winter mode (cf. Figs. 7 and 8), and from where future transformation can progress farther into the Arctic (toward the left in Fig. 7). The increasing “Atlantification” of the Barents Sea, Nansen basin, and eastern Eurasian basin (Årthun et al. 2012; Polyakov et al. 2017) is observational

evidence of transformation and consequently a seasonal ice cover moving poleward.

b. Future transformations from current change

A quantitative, if approximate, assessment of the future in line with the above space-for-time concept is the extrapolation of satellite-era regional trends for a representative summer (Chukchi Sea) and winter mode (Barents Sea) region. Linear trends since 1979 are considered (Fig. 7), same as for the sea ice extent trends updated monthly by the NSIDC (e.g., NSIDC 2016). We find that with the current observed Chukchi Sea summer loss rate ($-0.15 \times 10^6 \text{ km}^2 \text{ decade}^{-1}$; Fig. 4), the Chukchi Sea becomes ice free in summer during the 2020s and thus enters the transition mode (not shown). The estimate for the Chukchi Sea is also representative for the Laptev, Beaufort, and East Siberian Seas, as they have similar sea ice extent and trends (Figs. 3 and 4). These Arctic shelf seas may thus become seasonally ice free within the next decade, consistent with model projections of Arctic summer sea ice (e.g., Wang and Overland 2009).

We acknowledge that estimates based on extrapolation of linear trends are generically uncertain, particularly in a system that is rapidly changing (Meier et al. 2007). However, extrapolation on 1979–present trends can be considered a nonextreme estimate of future change; present shorter-term trends are distinctly larger (Fig. 5; Stroeve et al. 2012b), whereas climate models generally underestimate observed trends (Stroeve et al. 2012a). It is currently debated whether the latter mismatch reflects the models' imperfection in simulating externally forced change (from global warming), or the contribution of internal variability to observed trends (e.g., Li et al. 2017; Onarheim and Årthun 2017).

Given continued future warming, all the summer mode regions will eventually enter the transition mode and thus be ice free for parts of the year. Hudson Bay has currently approached the transition mode: it has practically no summer sea ice left, and is still completely ice covered in winter (Fig. 3). The corresponding monthly sea ice extent trends are thus large in fall and spring, but zero in summer and winter (Fig. 4) as the ocean is either completely ice free or fully ice covered. Also the Kara Sea has practically been ice free in recent summers and may thus be considered to be in a transition mode. The September trend in the Kara Sea (Fig. 4) is smaller than in the months prior to and after September. This indicates that there is limited September sea ice left to lose and that with continued warming the September sea ice extent trend decreases toward zero, as in the Hudson Bay and current winter mode regions.

Negative winter trends in the present winter mode regions will also persist in a climate that warms further, until these regions become ice free year-round. Here we assess the transformation from a winter ice-covered region to an ice-free sea exemplified by the Barents Sea ($-0.11 \times 10^6 \text{ km}^2 \text{ decade}^{-1}$; Fig. 4). As the winter sea ice extent loss progresses, larger open-water areas appear and the ice-free season lengthens. The Barents Sea becomes ice free year-round around 2050 if the currently observed winter trend in sea ice extent persists (not shown). This is in agreement with results from four CMIP5 models including a large ensemble simulation in a strong climate forcing scenario (Onarheim and Årthun 2017). The scenario of winter Barents Sea ice extent loss is also representative for the Greenland Sea, as it has similar sea ice extent and trends (Figs. 3 and 4), whereas the Sea of Okhotsk and Baffin Bay/Gulf of St. Lawrence are estimated to become ice free in the 2080s (not shown). We again note that the different regions are affected by different atmospheric and oceanic forcing; the partial sea ice cover in the Greenland Sea is for instance likely to persist as long as sea ice continues to be advected into the Greenland Sea from the Arctic Ocean (Kwok 2009).

8. Summary and conclusions

The NH sea ice cover has decreased dramatically over the past few decades, but with large seasonal and regional variations (Fig. 1). We note that only sea ice extent is considered herein, but that the observed decline in sea ice volume is also projected to continue toward 2100 (e.g., Gregory et al. 2002; Arzel et al. 2006). The observed NH sea ice extent variability and trend have here been assessed regionally and seasonally for the 1950–2016 period. Updated through 2016, changes are overall largest in summer and smallest in winter (e.g., Fig. 1) in agreement with previous studies (e.g., Cavalieri and Parkinson 2012). If the NH sea ice extent loss is to persist, summer trends will decrease as areas become ice free in summer, and trends toward the winter season will increase and spread to larger areas. On this background, we posed three questions initially (section 1): How are regional NH summer and winter sea ice extent variability and trends at present? How were they in the past? How may they be in the future?

Based on satellite observations, we propose two dominant patterns of NH sea ice extent variability and change, the summer and winter modes. The NH summer variability and trends dominate in the Arctic shelf seas (e.g., Figs. 2b and 5b). These regions are completely ice covered in winter but have large sea ice variability and trends in summer, and are thus classified to be in a

summer mode. The seas recently in summer mode are the central Arctic, Canadian Archipelago, the Beaufort, Chukchi, East Siberian, Laptev, and Kara Seas, and Hudson Bay. Current summer mode regions are characterized by larger trends in the melt season compared to the freezing season (Fig. 4), indicating that melt starts earlier whereas freeze-up happens relatively quickly. We find that the Arctic Ocean appears to refreeze particularly quickly—have rapid ice growth events—in years with a small sea ice extent minimum (Fig. 9).

The recent NH winter sea ice extent loss is significant and increasing, but still less extensive than in summer (Fig. 1; Cavalieri and Parkinson 2012). The winter variability and loss generally take place in the seas farther south, in the Barents Sea, Greenland Sea, Baffin Bay/Gulf of St. Lawrence, and Sea of Okhotsk (Fig. 2c). We classify these seas to be in a winter mode as they have largest sea ice extent variability and trends in winter. The Bering Sea is also placed within the winter mode, but has positive winter trends for the 1979–2016 period (Fig. 7). In contrast to the summer mode regions, the winter mode regions display similar trends in the freezing season compared to the melt season, and no rapid ice growth events are observed in fall.

Observations since 1950, although limited prior to the satellite era, indicate that the distinct summer (winter) mode regions explain large parts (>85% of the variance) of the NH summer (winter) sea ice extent variability (Fig. 6). With continued global warming and associated sea ice loss, however, regional seas may change from one mode to another. The summer mode regions may lose their summer sea ice, thereby transforming into a transition mode, and thereafter to the winter mode with sea ice variability and trends only in winter. The Kara Sea and Hudson Bay are currently about to leave the summer mode because they have lost nearly all summer sea ice (Figs. 3 and 9). By extrapolating current linear trends we find that the Arctic shelf seas in summer mode may become completely ice free in summer during the 2020s. Present winter variability and trend in sea ice extent within the Arctic Ocean occur exclusively in the Barents Sea (Fig. 2c). If the sea ice loss continues, the winter sea ice extent in the current summer mode regions may start decreasing and winter trends will then become increasingly important. Winter sea ice extent loss in the current winter mode regions will also persist with continued warming, until these regions become completely ice free throughout the year, possibly onward from the 2050s.

This work improves our understanding of past and present seasonal and regional NH sea ice extent variability by providing a unifying framework: the summer and winter modes. The modes highlight the ongoing

transformation and mark possible stages for the future seasonally ice-free Arctic Ocean.

Acknowledgments. This work was supported by the Centre for Climate Dynamics (SKD) at the Bjerknes Centre for Climate Research, the University of Bergen, and by the Research Council of Norway through the projects NORTH (project number 229763), EPOCASA (229774), and Nansen Legacy (272721). We thank three anonymous reviewers for their constructive suggestions that improved the manuscript.

REFERENCES

- Årthun, M., T. Eldevik, L. H. Smedsrud, Ø. Skagseth, and R. B. Ingvaldsen, 2012: Quantifying the influence of Atlantic heat on Barents Sea ice variability and retreat. *J. Climate*, **25**, 4736–4743, <https://doi.org/10.1175/JCLI-D-11-00466.1>.
- Arzel, O., T. Fichefet, and H. Goosse, 2006: Sea ice evolution over the 20th and 21st centuries as simulated by current AOGCMs. *Ocean Modell.*, **12**, 401–415, <https://doi.org/10.1016/j.ocemod.2005.08.002>.
- Beszczynska-Möller, A., E. Fahrbach, U. Schauer, and E. Hansen, 2012: Variability in Atlantic water temperature and transport at the entrance to the Arctic Ocean, 1997–2010. *ICES J. Mar. Sci.*, **69**, 852–863, <https://doi.org/10.1093/icesjms/fss056>.
- Cavalieri, D. J., and C. L. Parkinson, 1987: On the relationship between atmospheric circulation and the fluctuations in the sea ice extents of the Bering and Okhotsk seas. *J. Geophys. Res.*, **92**, 7141–7162, <https://doi.org/10.1029/JC092iC07p07141>.
- , and —, 2012: Arctic sea ice variability and trends, 1979–2010. *Cryosphere*, **6**, 881–889, <https://doi.org/10.5194/tc-6-881-2012>.
- , and Coauthors, 1992: NASA sea ice validation program for the DMSP SSM/I: Final Report. NASA Tech. Memo. 104559, 126 pp.
- , C. L. Parkinson, P. Gloersen, and H. Zwally, 1996: Sea ice concentrations from *Nimbus-7* SMMR and DMSP SSM/I passive microwave data, version 1. National Snow and Ice Data Center, accessed January 2017, <https://doi.org/10.5067/8GQ8LZQVLOVL>.
- , —, —, J. C. Comiso, and H. J. Zwally, 1999: Deriving long-term time series of sea ice cover from satellite passive-microwave multisensor data sets. *J. Geophys. Res.*, **104**, 15 803–15 814, <https://doi.org/10.1029/1999JC900081>.
- Chapman, W. L., and J. E. Walsh, 1991a: Arctic and Southern Ocean Sea Ice Concentrations, version 1. National Snow and Ice Data Center, <https://doi.org/10.7265/N5057CVT>.
- , and —, 1991b: Long-range prediction of regional sea ice anomalies in the Arctic. *Wea. Forecasting*, **6**, 271–288, [https://doi.org/10.1175/1520-0434\(1991\)006<0271:LRPORS>2.0.CO;2](https://doi.org/10.1175/1520-0434(1991)006<0271:LRPORS>2.0.CO;2).
- Close, S., M.-N. Houssais, and C. Herbaut, 2015: Regional dependence in the timing of onset of rapid decline in Arctic sea ice concentration. *J. Geophys. Res. Oceans*, **120**, 8077–8098, <https://doi.org/10.1002/2015JC011187>.
- , C. Herbaut, M.-N. Houssais, and A.-C. Blaizot, 2018: Mechanisms of interannual-to decadal-scale winter Labrador Sea ice variability. *Climate Dyn.*, <https://doi.org/10.1007/s00382-017-4024-z>, in press.
- Comiso, J. C., P. Wadhams, L. T. Pedersen, and R. A. Gersten, 2001: Seasonal and interannual variability of the Odden ice

- tongue and a study of environmental effects. *J. Geophys. Res.*, **106**, 9093–9116, <https://doi.org/10.1029/2000JC000204>.
- , C. L. Parkinson, R. Gersten, and L. Stock, 2008: Accelerated decline in the Arctic sea ice cover. *Geophys. Res. Lett.*, **35**, L01703, <https://doi.org/10.1029/2007GL031972>.
- Deser, C., J. E. Walsh, and M. S. Timlin, 2000: Arctic sea ice variability in the context of recent atmospheric circulation trends. *J. Climate*, **13**, 617–633, [https://doi.org/10.1175/1520-0442\(2000\)013<0617:ASIVIT>2.0.CO;2](https://doi.org/10.1175/1520-0442(2000)013<0617:ASIVIT>2.0.CO;2).
- Dickson, R., J. Lazier, J. Meincke, P. Rhines, and J. Swift, 1996: Long-term coordinated changes in the convective activity of the North Atlantic. *Prog. Oceanogr.*, **38**, 241–295, [https://doi.org/10.1016/S0079-6611\(97\)00002-5](https://doi.org/10.1016/S0079-6611(97)00002-5).
- Divine, D. V., and C. Dick, 2006: Historical variability of sea ice edge position in the Nordic seas. *J. Geophys. Res.*, **111**, C01001, <https://doi.org/10.1029/2004JC002851>.
- Emmerson, C., and G. Lahn, 2012: Arctic opening: Opportunity and risk in the high north. Lloyd's, 59 pp, http://library.arcticportal.org/1671/1/Arctic_Opening%2C_opportunity_and_risks_in_the_High_North.pdf.
- Fang, Z., and J. M. Wallace, 1994: Arctic sea ice variability on a timescale of weeks and its relation to atmospheric forcing. *J. Climate*, **7**, 1897–1914, [https://doi.org/10.1175/1520-0442\(1994\)007<1897:ASIVOA>2.0.CO;2](https://doi.org/10.1175/1520-0442(1994)007<1897:ASIVOA>2.0.CO;2).
- Francis, J. A., and S. J. Vavrus, 2012: Evidence linking Arctic amplification to extreme weather in mid-latitudes. *Geophys. Res. Lett.*, **39**, L06801, <https://doi.org/10.1029/2012GL051000>.
- Gagné, M.-È., J. C. Fyfe, N. P. Gillett, I. V. Polyakov, and G. M. Flato, 2017: Aerosol-driven increase in Arctic sea ice over the middle of the 20th century. *Geophys. Res. Lett.*, **44**, 7338–7346, <https://doi.org/10.1002/2016GL071941>.
- Gregory, J. M., P. A. Stott, D. J. Cresswell, N. A. Rayner, C. Gordon, and D. M. H. Sexton, 2002: Recent and future changes in Arctic sea ice simulated by the HadCM3 AOGCM. *Geophys. Res. Lett.*, **29**, 2175, <https://doi.org/10.1029/2001GL014575>.
- Honda, M., J. Inoue, and S. Yamane, 2009: Influence of low Arctic sea-ice minima on anomalously cold Eurasian winters. *Geophys. Res. Lett.*, **36**, L08707, <https://doi.org/10.1029/2008GL037079>.
- IPCC, 2013: *Climate Change 2013: The Physical Science Basis*. Cambridge University Press, 1535 pp., <https://doi.org/10.1017/CBO9781107415324>.
- Kashiwase, H., K. I. Ohshima, and S. Nihashi, 2014: Long-term variation in sea ice production and its relation to the intermediate water in the Sea of Okhotsk. *Prog. Oceanogr.*, **126**, 21–32, <https://doi.org/10.1016/j.pocean.2014.05.004>.
- Kay, J. E., M. M. Holland, and A. Jahn, 2011: Inter-annual to multi-decadal Arctic sea ice extent trends in a warming world. *Geophys. Res. Lett.*, **38**, L15708, <https://doi.org/10.1029/2011GL048008>.
- Kimura, N., and M. Wakatsuchi, 1999: Processes controlling the advance and retreat of sea ice in the Sea of Okhotsk. *J. Geophys. Res.*, **104**, 11 137–11 150, <https://doi.org/10.1029/1999JC900004>.
- Koenigk, T., M. Cai, G. Nikulin, and S. Schimanke, 2016: Regional Arctic sea ice variations as predictor for winter climate conditions. *Climate Dyn.*, **46**, 317–337, <https://doi.org/10.1007/s00382-015-2586-1>.
- Kwok, R., 2005: Variability of Nares Strait ice flux. *Geophys. Res. Lett.*, **32**, L24502, <https://doi.org/10.1029/2005GL024768>.
- , 2009: Outflow of Arctic Ocean sea ice into the Greenland and Barents Seas: 1979–2007. *J. Climate*, **22**, 2438–2457, <https://doi.org/10.1175/2008JCLI2819.1>.
- , and D. Rothrock, 2009: Decline in Arctic sea ice thickness from submarine and ICESat records: 1958–2008. *Geophys. Res. Lett.*, **36**, L15501, <https://doi.org/10.1029/2009GL039035>.
- Li, D., R. Zhang, and T. R. Knutson, 2017: On the discrepancy between observed and CMIP5 multi-model simulated Barents Sea winter sea ice decline. *Nat. Commun.*, **8**, 14991, <https://doi.org/10.1038/ncomms14991>.
- Lindsay, R. W., and J. Zhang, 2005: The thinning of Arctic sea ice, 1988–2003: Have we passed a tipping point? *J. Climate*, **18**, 4879–4894, <https://doi.org/10.1175/JCLI3587.1>.
- Mahoney, A. R., R. G. Barry, V. Smolyanitsky, and F. Fetterer, 2008: Observed sea ice extent in the Russian Arctic, 1933–2006. *J. Geophys. Res.*, **113**, C11005, <https://doi.org/10.1029/2008JC004830>.
- Martin, S., R. Drucker, and K. Yamashita, 1998: The production of ice and dense shelf water in the Okhotsk Sea polynyas. *J. Geophys. Res.*, **103**, 27 771–27 782, <https://doi.org/10.1029/98JC02242>.
- Maslanik, J. A., M. C. Serreze, and T. Agnew, 1999: On the record reduction in 1998 western Arctic sea-ice cover. *Geophys. Res. Lett.*, **26**, 1905–1908, <https://doi.org/10.1029/1999GL900426>.
- , C. Fowler, J. Stroeve, S. Drobot, J. Zwally, D. Yi, and W. Emery, 2007: A younger, thinner Arctic ice cover: Increased potential for rapid, extensive sea-ice loss. *Geophys. Res. Lett.*, **34**, L24501, <https://doi.org/10.1029/2007GL032043>.
- Meier, W., J. Stroeve, F. Fetterer, and K. Knowles, 2005: Reductions in Arctic sea ice cover no longer limited to summer. *Eos, Trans. Amer. Geophys. Union*, **86**, 326–326, <https://doi.org/10.1029/2005EO360003>.
- , —, and —, 2007: Whither Arctic sea ice? A clear signal of decline regionally, seasonally and extending beyond the satellite record. *Ann. Glaciol.*, **46**, 428–434, <https://doi.org/10.3189/172756407782871170>.
- , F. Fetterer, M. Savoie, S. Mallory, R. Duerr, and J. Stroeve, 2013: NOAA/NSIDC climate data record of passive microwave sea ice concentration, version 2. National Snow and Ice Data Center, <https://doi.org/10.7265/N55M63M1>.
- Muench, R. D., and K. Ahlnas, 1976: Ice movement and distribution in the Bering Sea from March to June 1974. *J. Geophys. Res.*, **81**, 4467–4476, <https://doi.org/10.1029/JC081i024p04467>.
- Nghiem, S. V., I. G. Rigor, D. Perovich, P. Clemente-Colón, J. W. Weatherly, and G. Neumann, 2007: Rapid reduction of Arctic perennial sea ice. *Geophys. Res. Lett.*, **34**, L19504, <https://doi.org/10.1029/2007GL031138>.
- Notz, D., and J. Marotzke, 2012: Observations reveal external driver for Arctic sea-ice retreat. *Geophys. Res. Lett.*, **39**, L08502, <https://doi.org/10.1029/2012GL051094>.
- , and J. Stroeve, 2016: Observed Arctic sea-ice loss directly follows anthropogenic CO₂ emission. *Science*, **354**, 747–750, <https://doi.org/10.1126/science.aag2345>.
- NSIDC, 2016: Rapid ice growth follows the seasonal minimum, rapid drop in Antarctic extent. *Arctic Sea Ice News & Analysis*, <http://nsidc.org/arcticseaicenews/2016/10/>.
- Ogi, M., and J. M. Wallace, 2012: The role of summer surface wind anomalies in the summer Arctic sea ice extent in 2010 and 2011. *Geophys. Res. Lett.*, **39**, L09704, <https://doi.org/10.1029/2012GL051330>.
- Onarheim, I. H., and M. Årthun, 2017: Toward an ice-free Barents Sea. *Geophys. Res. Lett.*, **44**, 8387–8395, <https://doi.org/10.1002/2017GL074304>.
- , L. H. Smedsrud, R. B. Ingvaldsen, and F. Nilsen, 2014: Loss of sea ice during winter north of Svalbard. *Tellus*, **66A**, 23933, <https://doi.org/10.3402/tellusa.v66.23933>.

- , T. Eldevik, M. Årthun, R. B. Ingvaldsen, and L. H. Smedsrud, 2015: Skillful prediction of Barents Sea ice cover. *Geophys. Res. Lett.*, **42**, 5364–5371, <https://doi.org/10.1002/2015GL064359>.
- Perovich, D. K., B. Light, H. Eicken, K. F. Jones, K. Runciman, and S. V. Nghiem, 2007: Increasing solar heating of the Arctic Ocean and adjacent seas, 1979–2005: Attribution and role in the ice-albedo feedback. *Geophys. Res. Lett.*, **34**, L19505, <https://doi.org/10.1029/2007GL031480>.
- Polyakov, I. V., and Coauthors, 2003: Long-term ice variability in Arctic marginal seas. *J. Climate*, **16**, 2078–2085, [https://doi.org/10.1175/1520-0442\(2003\)016<2078:LIVIAM>2.0.CO;2](https://doi.org/10.1175/1520-0442(2003)016<2078:LIVIAM>2.0.CO;2).
- , and Coauthors, 2017: Greater role for Atlantic inflows on sea-ice loss in the Eurasian Basin of the Arctic Ocean. *Science*, **356**, 285–291, <https://doi.org/10.1126/science.aai8204>.
- Rampal, P., J. Weiss, and D. Marsan, 2009: Positive trend in the mean speed and deformation rate of Arctic sea ice, 1979–2007. *J. Geophys. Res.*, **114**, C05013, <https://doi.org/10.1029/2008JC005066>.
- Rawlins, M. A., and Coauthors, 2010: Analysis of the Arctic system for freshwater cycle intensification: Observations and expectations. *J. Climate*, **23**, 5715–5737, <https://doi.org/10.1175/2010JCLI3421.1>.
- Rigor, I. G., J. M. Wallace, and R. L. Colony, 2002: Response of sea ice to the Arctic Oscillation. *J. Climate*, **15**, 2648–2663, [https://doi.org/10.1175/1520-0442\(2002\)015<2648:ROSITT>2.0.CO;2](https://doi.org/10.1175/1520-0442(2002)015<2648:ROSITT>2.0.CO;2).
- Rudels, B., 2015: Arctic Ocean circulation, processes and water masses: A description of observations and ideas with focus on the period prior to the International Polar Year 2007–2009. *Prog. Oceanogr.*, **132**, 22–67, <https://doi.org/10.1016/j.pocean.2013.11.006>.
- , D. Quadfasel, H. Friedrich, and M.-N. Houssais, 1989: Greenland Sea convection in the winter of 1987–1988. *J. Geophys. Res.*, **94**, 3223–3227, <https://doi.org/10.1029/JC094iC03p03223>.
- Screen, J. A., 2017: Simulated atmospheric response to regional and pan-Arctic sea ice loss. *J. Climate*, **30**, 3945–3962, <https://doi.org/10.1175/JCLI-D-16-0197.1>.
- Serreze, M. C., and R. G. Barry, 2011: Processes and impacts of Arctic amplification: A research synthesis. *Global Planet. Change*, **77**, 85–96, <https://doi.org/10.1016/j.gloplacha.2011.03.004>.
- , M. M. Holland, and J. Stroeve, 2007: Perspectives on the Arctic's shrinking sea-ice cover. *Science*, **315**, 1533–1536, <https://doi.org/10.1126/science.1139426>.
- Shimada, K., T. Kamoshida, M. Itoh, S. Nishino, E. Carmack, F. McLaughlin, S. Zimmermann, and A. Proshutinsky, 2006: Pacific Ocean inflow: Influence on catastrophic reduction of sea ice cover in the Arctic Ocean. *Geophys. Res. Lett.*, **33**, L08605, <https://doi.org/10.1029/2005GL025624>.
- Smedsrud, L. H., and Coauthors, 2013: The role of the Barents Sea in the Arctic climate system. *Rev. Geophys.*, **51**, 415–449, <https://doi.org/10.1002/rog.20017>.
- , M. H. Halvorsen, J. C. Stroeve, R. Zhang, and K. Kloster, 2017: Fram Strait sea ice export variability and September Arctic sea ice extent over the last 80 years. *Cryosphere*, **11**, 65–79, <https://doi.org/10.5194/tc-11-65-2017>.
- Steele, M., and S. Dickinson, 2016: The phenology of Arctic Ocean surface warming. *J. Geophys. Res. Oceans*, **121**, 6847–6861, <https://doi.org/10.1002/2016JC012089>.
- Stroeve, J. C., V. Kattsov, A. Barrett, M. Serreze, T. Pavlova, M. Holland, and W. N. Meier, 2012a: Trends in Arctic sea ice extent from CMIP5, CMIP3 and observations. *Geophys. Res. Lett.*, **39**, L16502, <https://doi.org/10.1029/2012GL052676>.
- , M. C. Serreze, M. M. Holland, J. E. Kay, J. Malanik, and A. P. Barrett, 2012b: The Arctic's rapidly shrinking sea ice cover: A research synthesis. *Climatic Change*, **110**, 1005–1027, <https://doi.org/10.1007/s10584-011-0101-1>.
- , T. Markus, L. Boisvert, J. Miller, and A. Barrett, 2014: Changes in Arctic melt season and implications for sea ice loss. *Geophys. Res. Lett.*, **41**, 1216–1225, <https://doi.org/10.1002/2013GL058951>.
- Titchner, H. A., and N. A. Rayner, 2014: The Met Office Hadley Centre sea ice and sea surface temperature data set, version 2: 1. Sea ice concentrations. *J. Geophys. Res. Atmos.*, **119**, 2864–2889, <https://doi.org/10.1002/2013JD020316>.
- Vinje, T., 2001: Anomalies and trends of sea-ice extent and atmospheric circulation in the Nordic seas during the period 1864–1998. *J. Climate*, **14**, 255–267, [https://doi.org/10.1175/1520-0442\(2001\)014<0255:AATOSI>2.0.CO;2](https://doi.org/10.1175/1520-0442(2001)014<0255:AATOSI>2.0.CO;2).
- Wadhams, P., and J. C. Comiso, 1999: Two modes of appearance of the Odden ice tongue in the Greenland Sea. *Geophys. Res. Lett.*, **26**, 2497–2500, <https://doi.org/10.1029/1999GL900502>.
- Walsh, J. E., and C. M. Johnson, 1979: An analysis of Arctic sea ice fluctuations, 1953–77. *J. Phys. Oceanogr.*, **9**, 580–591, [https://doi.org/10.1175/1520-0485\(1979\)009<0580:AAOASI>2.0.CO;2](https://doi.org/10.1175/1520-0485(1979)009<0580:AAOASI>2.0.CO;2).
- , W. L. Chapman, and F. Fetterer, 2015: Gridded monthly sea ice extent and concentration, 1850 onward, version 1. National Snow and Ice Data Center, Boulder, CO, accessed January 2016, <http://dx.doi.org/10.7265/N5833PZ5>.
- , F. Fetterer, J. S. Stewart, and W. L. Chapman, 2017: A database for depicting Arctic sea ice variations back to 1850. *Geogr. Rev.*, **107**, 89–107, <https://doi.org/10.1111/j.1931-0846.2016.12195.x>.
- Wang, M., and J. E. Overland, 2009: A sea ice free summer Arctic within 30 years? *Geophys. Res. Lett.*, **36**, L07502, <https://doi.org/10.1029/2009GL037820>.
- Williams, J., B. Tremblay, R. Newton, and R. Allard, 2016: Dynamic preconditioning of the minimum September sea-ice extent. *J. Climate*, **29**, 5879–5891, <https://doi.org/10.1175/JCLI-D-15-0515.1>.
- Woodgate, R. A., K. Aagaard, and T. J. Weingartner, 2006: Interannual changes in the Bering Strait fluxes of volume, heat and freshwater between 1991 and 2004. *Geophys. Res. Lett.*, **33**, L15609, <https://doi.org/10.1029/2006GL026931>.